Ann. Geophys., 27, 2869–2879, 2009
www.ann-geophys.net/27/2869/2009/
© Author(s) 2009. This work is distributed under
the Creative Commons Attribution 3.0 License.

Annales Geophysicae

# Transport of dust and anthropogenic aerosols across Alexandria, Egypt

**H. El-Askary**[1,2,3,4], **R. Farouk**[3], **C. Ichoku**[5], **and M. Kafatos**[1,2]

[1]Department of Physics Computational Science, and Engineering, Schmid College of Science, Chapman University, Orange, CA 92866, USA
[2]Center of Excellence in Earth Observing, Chapman University, Orange, CA 92866, USA
[3]Department of Environmental Sciences, Faculty of Science, Alexandria University, Moharem Bek, Alexandria, 21522, Egypt
[4]National Authority for Remote Sensing and Space Science (NARSS), Cairo, Egypt
[5]Climate & Radiation Branch, Code 613.2, NASA Goddard Space Flight Center, Greenbelt, MD 20771, USA

Received: 24 March 2009 – Revised: 21 June 2009 – Accepted: 7 July 2009 – Published: 21 July 2009

**Abstract.** The flow of pollutants from Europe and desert dust to Europe from the Sahara desert both affects the air quality of the coastal regions of Egypt. As such, measurements from both ground and satellite observations assume great importance to ascertain the conditions and flow affecting the Nile Delta and the large city of Alexandria. We note that special weather conditions prevailing in the Mediterranean Sea result in a westerly wind flow pattern during spring and from North to South during the summer. Such flow patterns transport dust-loaded and polluted air masses from the Sahara desert and Europe, respectively, through Alexandria, and the Nile Delta in Egypt. We have carried out measurements acquired with a ground- based portable sun photometer (Microtops II) and the satellite-borne TERRA/Moderate Resolution Imaging Spectroradiometer (MODIS) sensor during the periods of October 1999–August 2001 and July 2002–September 2003. These measurements show a seasonal variability in aerosol optical depth (AOD) following these flow patterns. Maximum aerosol loadings accompanied by total precipitable water vapor (W) enhancements are observed during the spring and summer seasons. Pronounced changes have been observed in the Ångström exponent ($\alpha$) derived from ground-based measurements over Alexandria (31.14° N, 29.59° E) during both dust and pollution periods. We have followed up the observations with a 3-day back-trajectories model to trace the probable sources and pathways of the air masses causing the observed aerosol loadings. We have also used other NASA model outputs to estimate the sea salt, dust, sulfates and black carbon AOD spatial distributions during different seasons. Our results reveal the probable source regions of these aerosol types, showing agreement with the trajectory and Ångström exponent analysis results. It is confirmed that Alexandria is subjected to different atmospheric conditions involving dust, pollution, mixed aerosols and clean sky.

**Keywords.** Atmospheric composition and structure (Aerosols and particles; Pollution – urban and regional)

*Correspondence to:* H. El-Askary
(elaskary@chapman.edu)

## 1 Introduction

Egypt is influenced by the regional scale trade wind system caused by differential heating between the Mediterranean Sea and the land regions of North Africa (bare and dry) and Southern Europe (partial vegetation coverage). This system is enhanced during the warm period of the year by the strong gradient between the Atlantic anticyclone activity and monsoon activity over the Indian Ocean and Middle East. The resulting circulation patterns over Egypt are winds from North that enhance the sea breezes along the North African coastline. This flow regime penetrates deep inside Egypt and assists in cleaning the air in the urban locations within the greater Delta region, such as Cairo, Alexandria, and adjoining areas

(Kallos et al., 1998, 2007). The boundary layer height changes from a few hundred meters at night to 2–4 km during daytime, thus also assisting in pumping local air pollutants away from their sources (Kallos et al., 1998). During fall, this pattern is weakened significantly and local circulations start to develop, while stagnation, local boundary layer formation along the coast, and shallow boundary layer formations in general, are the characteristics that lead to poor pollutant dispersion conditions. Also, during fall, biomass burning in the greater Nile Delta becomes a major contributor

to local air quality degradation due to poor ventilation processes (e.g. light winds and shallow boundary layer).

Past studies have identified the pathways and scales of transport and transformation of air pollutants released from Europe towards the Eastern Mediterranean and North Africa (Luria et al., 1996; Millan et al., 1997; Kallos et al., 1998). Emissions of atmospheric constituents from the African continent include both trace gases and aerosols. These emissions are derived from windblown dust, biomass burning, biogenic emissions and anthropogenic industrial activities (Piketh and Walton, 2004). Over the Eastern Mediterranean region, models predict that sulfate aerosols contribute to the net direct radiative forcing (Charlson et al., 1991; Kiehl and Rodhe, 1995). For that reason, many experimental aerosol studies have targeted that region over the last decade (Andreae et al., 2002; El-Metwally et al., 2008; Gerasopoulos et al., 2003; Ichoku et al., 1999; Kambezidis and Kaskaoutis, 2008; Kaskaoutis et al., 2007 and 2008; Kouvarakis et al., 2002; Lelieveld et al., 2002; Luria et al., 1996; Meloni et al., 2008; Pinker et al., 1997; Paronis et al., 1998).

The objective of the current study is to investigate the regional pattern of pollution and dust aerosols exchange from and to Europe. Dust is predominantly emitted from Sahara desert, which is the major source of dust in this region. The current study investigates a multi-year remotely sensed aerosol data acquired from both MODIS sensor and ground Microtops II sun photometer, over Alexandria, Egypt, which is centrally situated within the region of interest. Alexandria is the second largest city in Egypt, and houses more than 60% of the Egyptian national industries. It lies at the junction of several weather systems, including the Mediterranean and the Saharan ones. As a result, it is characterized by a complex synoptic meteorology, which follows an annual cycle (Moulin et al., 1998).

## 2 Instrumentation, data and methodology

In this research, ground-based aerosol remote sensing was conducted using a portable Microtops II sun photometer manufactured by Solar Light Co., USA. The Sun photometer measures solar radiance ($\mathrm{W\,sr^{-1}m^{-2}}$) in five spectral wave bands (340, 440, 675, 870, and 936 nm) from which the spectral aerosol optical depth (AOD) is derived. Since the 936 nm wavelength is greatly affected by water-vapor absorption, it is used to derive the total water- vapor column amount, $W$. The derived AOD and $W$ data were subsequently adjusted following calibration processes performed as described by Ichoku et al. (2002). The absolute accuracy of the calibration-adjusted AOD measurements is expected to be $\pm 0.02$ over the mean, with precision 4 times better than that of the corresponding values before adjustment (Sabbah et al., 2001).

Microtops II sun photometer measurements were conducted for several years, on clear days when no cloud patch was even close to the sun, to avoid cloud contamination. For better quality control, measurements were taken in triplets. One or several such sets of measurements were obtained per day. Approximately once per year, the sun photometer was returned to the National Aeronautics and Space Administration (NASA), Goddard Space Flight Center (GSFC), Greenbelt, Maryland, USA, and calibrated against a reference instrument, which is the master automatic tracking sun photometer/sky radiometer (CIMEL Electronique 318A) belonging to AERONET (Holben et al., 1998). The calibration enabled the determination of calibration coefficients used for the adjustment of all data acquired between two successive calibrations. Overall, the data used in this work were obtained from 19 October 1999 to 20 August 2001, and from 28 July 2002 to 4 September 2003.

The spectral AOD at a given wavelength $\lambda$ ($\tau_\lambda$) represents the extinction of radiation at wavelength $\lambda$ as a result of the presence of atmospheric aerosols. AOD measurements in two adjacent wavelengths can be used to calculate the corresponding Ångström exponent ($\alpha$) given in Eq. (1), which represents the slope of the wavelength dependence of the AOD in logarithmic coordinates (Ångström, 1929).

$$\alpha(\lambda_1, \lambda_2) = -\ln\left(\frac{\tau_{\lambda_2}}{\tau_{\lambda_1}}\right) \Big/ \ln\left(\frac{\lambda_2}{\lambda_1}\right) \quad (1)$$

In the solar spectrum, $\alpha$ is a good indicator of the size range of the atmospheric particles responsible for the AOD: $\alpha > 1$ when fine mode (submicron) aerosols are dominant, while $\alpha < 1$ for aerosols dominated by coarse or supermicron particles. In fact, King et al. (1978), Nakajima et al. (1986), Kaufman (1993), Eck et al. (1999), O'Neill et al. (2001a, b, 2003), Schuster et al. (2006) and Gobbi et al. (2007) discuss how the spectral variation of the Ångström exponent can provide further information about the aerosol-size distribution. Many satellite-based and ground-based measurements provide retrievals of spectral AOD, but no direct size-distribution retrievals. Therefore, analysis of $\alpha$ is important in the interpretation of these data and in providing further information on particle size.

## 3 Aerosol (pollution/dust) discrimination using Ångström exponent

A study of the aerosol parameters during major dust storm events (2001–2005) over the Indo-Gangetic (IG) Plains, India (Prasad and Singh, 2007) shows a large increase in AOD from 0.4–0.6 to more than 1, and a corresponding sharp decline in the Ångström exponent (to the 0–0.4 range) with the arrival of dust storms compared to non-dusty days. A sharp decrease in the Ångström exponent to low and even negative values was observed over Delhi and Hyderabad during dust storm events (Badarinath et al., 2007; Singh et al., 2005) and also during Saharan dust events (Kaskaoutis et al., 2008; Hamonou et al., 1999). An enhanced level of $W$ ($>3$ cm, in near

infra-red, clear column) has been found to be associated with higher aerosol loading during these dust storms.

Aerosols over the Northern coast of Egypt can have both local and distant origins depending on the season. Aerosols from local sources may either be from natural causes, for instance desert dust particles directly transported from the Western desert regions or maritime particles produced over the Mediterranean; or anthropogenic emissions from the Alexandria industrialized areas and smoke particles from seasonal biomass fires over the Greater Delta region (e.g. Barnaba and Gobbi, 2004). This area is also exposed to long-range transport of not only the Saharan dust, but also anthropogenic pollutants (mainly from Europe) (Luria et al., 1996; Millan et al., 1997; and Kallos et al., 1998, 2007). According to their findings, long-range transported anthropogenic aerosol concentrations are very high during the warm period of the year due to the prevailing trade wind patterns, photochemical activity, and the absence of precipitation. Desert dust transport is a major contributor during the spring and the transitional seasons. Sea-salt particles contribute to aerosol concentrations over the coastal areas, mainly during strong wind weather conditions (synoptic scale component). Sea salt becomes more important during winter due to the passage of synoptic systems and during summer due to trade winds from the north and associated wave breaking activity along the coastline. Knowledge of these seasonal patterns can be combined with the aerosol Ångström exponent $\alpha$ analysis to achieve an approximate differentiation of the aerosols' origins. In this study, $\alpha$ was determined from AOD measurements at 675 nm and 440 nm wavelengths as given in Eq. (2) following Ichoku et al. (2002).

$$\alpha_{675/440} = -\frac{\ln(\tau_{a675}/\tau_{a440})}{\ln(675/440)} \quad (2)$$

where, $\alpha_{675/440}$ is the Ångström exponent derived using only the AOD values ($\tau_{a675}$ and $\tau_{a440}$) measured at the 675 and 440 nm channels. These two wavelengths have been used because the computed $\alpha_{675/440}$ can be used to interpolate $\tau_{a550}$, which can then be plotted together with equivalent MODIS values. Also, the closeness of this wavelength pair allows us to avoid the curvature in spectral dependence described by Eck et al. (1999).

High $\alpha$ values indicate a higher abundance of smaller aerosol particles, while low $\alpha$ ones reflect coarser particle sizes. The coarse-mode aerosols are mainly from sea salt and mineral dust, whereas the mainly anthropogenic submicron aerosols are mostly carbonaceous and sulfate aerosols generated from biomass burning and urban/industrial activities in addition to those from gas-to-particle conversion mechanisms (Ramachandran, 2004). Therefore, either an increase in the number of smaller particles or a decrease in the number of larger particles can cause an increase in the value of $\alpha$. In that context, we classified the months into different categories (clean/dust/pollution/mixed) according to the number of days that fall into each. This categorization is based on the AOD $\tau_{a675}$ values and the Ångström exponent $\alpha_{675/440}$ (Sabbah et al., 2001). Cases with $\tau_{a675} \leq 0.06$ were classified as "clean" conditions. For those with $\tau_{a675} > 0.06$, further classification was based on the values of the Ångström exponent, being categorized as "dust" for $\alpha_{675/440} < 0.25$, "pollution" for $\alpha_{675/440} > 1.0$, and "mixed" otherwise (Table 1).

**Table 1.** Percentages of occurrence for different aerosol categories and their corresponding Ångström exponent.

| Month | Dust (%) | Pollution (%) | Clean (%) | Mixed (%) | $\alpha$675/440 |
|---|---|---|---|---|---|
| Oct 1999 | 23.1 | 15.4 | 7.7 | 53.8 | 0.61 |
| Nov 1999 | 19.2 | 30.8 | 11.5 | 38.5 | 0.88 |
| Dec 1999 | 24.0 | 12.0 | 0.0 | 64.0 | 0.90 |
| Jan 2000 | 26.3 | 10.5 | 5.3 | 57.9 | 0.68 |
| Feb 2000 | 26.1 | 17.4 | 0.0 | 56.5 | 0.87 |
| Mar 2000 | 25.0 | 3.6 | 0.0 | 71.4 | 0.70 |
| Apr 2000 | 34.5 | 10.3 | 0.0 | 55.2 | 0.62 |
| May 2000 | 3.6 | 10.7 | 21.4 | 64.3 | 1.03 |
| Jun 2000 | 0.0 | 26.7 | 13.3 | 60.0 | 1.29 |
| Jul 2000 | 25.8 | 25.8 | 3.2 | 45.2 | 0.59 |
| Aug 2000 | 0.0 | 66.7 | 6.7 | 26.7 | 1.41 |
| Sep 2000 | 0.0 | 36.7 | 0.0 | 63.3 | 1.12 |
| Oct 2000 | 0.0 | 50.0 | 7.1 | 42.9 | 1.19 |
| Nov 2000 | 0.0 | 58.3 | 0.0 | 41.7 | 1.24 |
| Dec 2000 | 11.1 | 33.3 | 11.1 | 44.4 | 0.96 |
| Jan 2001 | 25.0 | 35.7 | 10.7 | 28.6 | 1.04 |
| Feb 2001 | 17.4 | 21.7 | 4.3 | 56.5 | 0.88 |
| Mar 2001 | 32.0 | 0.0 | 4.0 | 64.0 | 0.63 |
| Apr 2001 | 52.2 | 8.7 | 8.7 | 30.4 | 0.37 |
| May 2001 | 50.0 | 9.1 | 0.0 | 40.9 | 0.46 |
| Jun 2001 | 10.0 | 3.3 | 6.7 | 80.0 | 0.97 |
| Jul 2001 | 10.0 | 15.0 | 0.0 | 75.0 | 0.96 |
| Aug 2001 | 0.0 | 33.3 | 0.0 | 66.7 | 1.16 |
| Aug 2002 | 6.9 | 51.7 | 0.0 | 41.4 | 0.89 |
| Sep 2002 | 17.2 | 31.0 | 0.0 | 51.7 | 0.69 |
| Oct 2002 | 6.7 | 36.7 | 0.0 | 56.7 | 0.85 |
| Nov 2002 | 11.5 | 46.2 | 7.7 | 34.6 | 0.87 |
| Dec 2002 | 13.0 | 34.8 | 0.0 | 52.2 | 0.76 |
| Jan 2003 | 24.1 | 27.6 | 13.8 | 34.5 | 0.48 |
| Feb 2003 | 19.0 | 9.5 | 0.0 | 71.4 | 0.47 |
| Mar 2003 | 8.7 | 47.8 | 0.0 | 43.5 | 0.83 |
| Apr 2003 | 29.2 | 29.2 | 0.0 | 41.7 | 0.42 |
| May 2003 | 4.0 | 20.0 | 0.0 | 76.0 | 0.67 |
| Jun 2003 | 0.0 | 74.1 | 0.0 | 25.9 | 1.11 |
| Jul 2003 | 0.0 | 65.5 | 0.0 | 34.5 | 1.09 |
| Aug 2003 | 0.0 | 75.9 | 3.4 | 20.7 | 1.18 |

## 4 Inferring aerosol seasonality

A time-series analysis of the frequency of occurrence of the four pre-defined aerosol categories, together with monthly

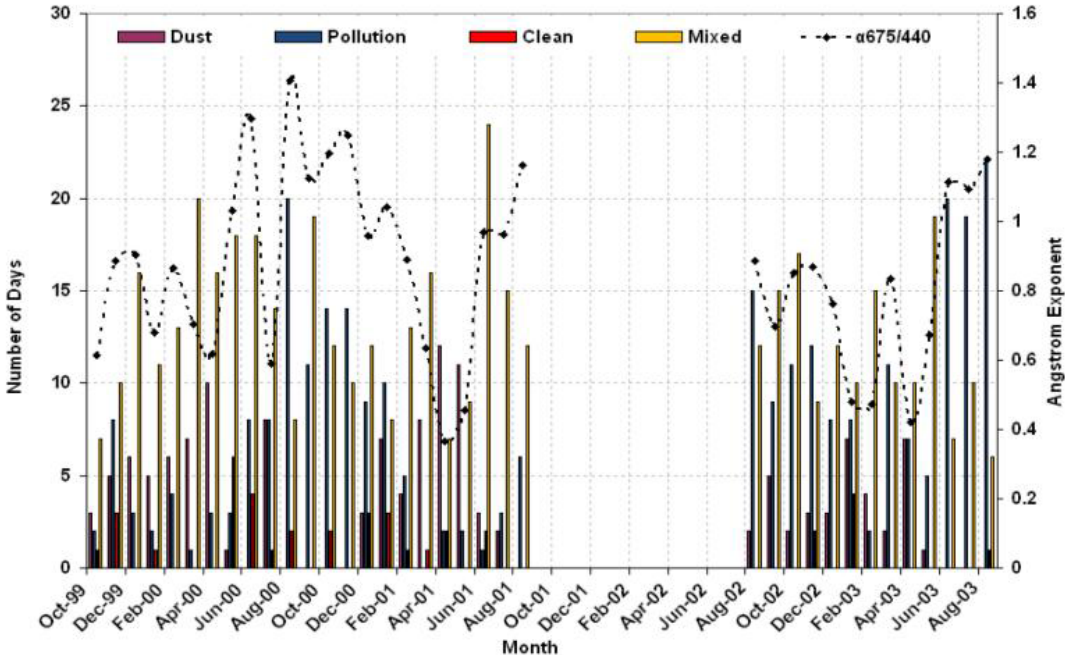


**Fig. 1.** Number of days with measurements and occurrences for different aerosol categories and their corresponding Ångström exponent over Alexandria for two time periods from October 1999 to August 2001 and from August 2002 to August 2003.

averages of the AOD, precipitable water vapor ($W$), and the Ångström exponent ($\alpha_{675/440}$) from Microtops II, combined with MODIS-derived AOD and aerosol fine mode fraction (FMF) over Alexandria, as well as fire detections in the Greater Nile Delta region, can provide some insight into the pattern and seasonality of aerosol transport and its potential impacts. The time-series plot of the relative fraction for each month dominated by each aerosol category (Fig. 1) shows a data gap, when the Microtops II sunphotometer was sent to NASA for an extended period (between August 2001 and August 2002) for calibration. The accuracy of the MODIS AOD Collection 005 data used in this study has been discussed in detail by Levy et al. (2007).

During the first data period, the months with the highest frequency of days with dust events were April 2001 (52.2%), May 2001 (50.0%), April 2000 (34.5%), and March 2001 (32.0%). However, during the second time period, the highest dust percentages were in April 2003 (29.2%), January 2003 (24.1%), February 2003 (19.0%), and September 2002 (17.2%). It is clear that April is the month with the most frequent dust event occurrences in Alexandria (khamaseen storms), and is probably the peak month for transport of Saharan dust to the Near East and Eastern Europe. In terms of the monthly mean AOD (Fig. 3), the peak months during these dust seasons were April 2000, May 2001, and April 2003. Incidentally, the April 2000 and May 2001 dust peaks coincide with $W$ peaks, which may have provided favorable conditions for cloud seeding and nucleation, with the possible enhancement of indirect radiative forcing (El-Askary et al., 2003). El-Askary et al. (2006, 2008) observed a slowly increasing water-vapor column from March through May in 2000, 2001 and 2003. However, they found that the highest water-vapor column value observed during spring is still lower than the values found during September through November. July generally represents a dust free month, but in July 2000 the dust occurrence percentage was 25.8% (see Fig. 1 and Table 1), which is significantly high for this period of the year. The presence of dust produces a noticeable dip in the Ångström exponent value, but also causes an enhancement in the monthly mean AOD value, which is showing as a peak in the time-series (Fig. 2). This unusual dust outbreak during the month of July in the Southeastern Mediterranean region in 2000 was also reported by Alpert et al. (2002), who suggested that a strong dry convection that may have developed over the Saharan source regions may have lifted the dust to a high altitude (say above 700 hPa), thereby allowing the upper-level southwesterly winds to transport the dust northeastward over the Southeastern Mediterranean region. This observation agrees with the findings reported by Kaskaoutis et al. (2008). It is also noteworthy that the synoptic systems prevailing during this period and responsible for dust transport are the "North African Depressions" that move along the coast of North Africa towards Middle East that have as a result the transport of dust from Sahara towards the Mediterranean.

As regards to the pollution episodes, it was found (Fig. 1) that during the first period, the months with the most pollution days were August 2000 (66.7%), November 2000

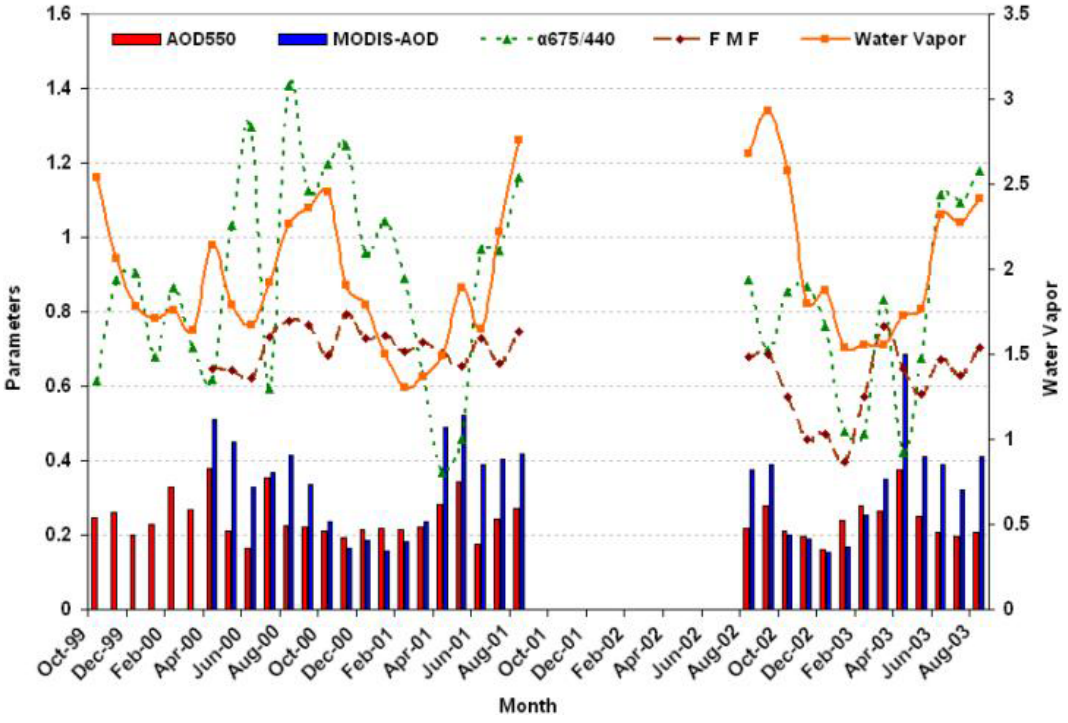


**Fig. 2.** Microtops II monthly mean AOD at (550 nm), precipitable water vapor and Ångström exponent ($\alpha$675/440) with corresponding monthly means of MODIS-AOD and FMF over Alexandria for two time periods from October 1999 to August 2001 and from August 2002 to August 2003.

(58.3%), October 2000 (50.0%) and September 2000 (36.7%). However, during the second time period, the highest pollution months were August 2003 (75.9%), June 2003 (74.1%), July 2003 (65.5%), and August 2002 (51.7%). These summer-fall months have been known to be the dominant pollution months in this region (El-Askary et al., 2006, 2008). They are also associated with high $W$ amounts (Fig. 2), thereby providing conditions favorable to indirect radiative forcing by anthropogenic aerosols.

Since smoke is also included producing high $\alpha$-values, an attempt was made to determine the influence of smoke from the biomass burning within the Greater Nile Delta region on these pollution peaks. Fire pixel counts were obtained from MODIS on the Terra satellite, and the total counts per month were calculated and plotted (Fig. 3) for the study period. Based on these data, peak biomass burning was found to occur in September (2001 and 2002) or October (2003 and 2004). Nevertheless, it could be inferred that fine-particles were the dominant aerosols from local biomass burning in the Egyptian Nile delta peaks in September or October, and may be partly responsible for the peak pollution found in September–October 2000 (El-Askary et al., 2006, 2008). Since there is virtually no biomass burning in the locality at other times of the year, it is probable that the rest of the peaks in the pollution category observed from the monthly frequency data may have been due to long- range transport from the Near East and Southeastery Europe. Hence, high AOD values during April–May are attributed to large dust loading in the atmosphere, while FMF shows high values during the summer and fall seasons due to the urban/industrial and bio-fuel emissions. It is noteworthy that MODIS AOD values seem to be higher than the ground observations in the summer-fall months for reasons relating to the complexity of satellite retrieval of mixed aerosols over coastal semi-arid land surfaces (Remer et al., 2005).

## 5 Model analysis of aerosol transport

For better understanding of the aerosol-transport patterns in the study region, we have used the NOAA Air Resources Laboratory (ARL) HYSPLIT_4 model (Draxler and Hess, 1998; Draxler, 1999) to generate air-mass back trajectories over Alexandria for selected days, in order to investigate the probable sources of the different aerosol types. Also, Goddard Chemistry Aerosol Radiation and Transport (GOCART) model (Chin et al., 2000) outputs were obtained to determine the possible sources and spatial distribution of sea salt, dust, sulfates and black-carbon AOD over Alexandria and the surrounding delta region during the four seasons of 2003. Table 2 shows the daily average AOD measurements at 675 nm, $\alpha_{675/440}$, $W$, the aerosol type, for the selected days representing the four scenarios addressed,

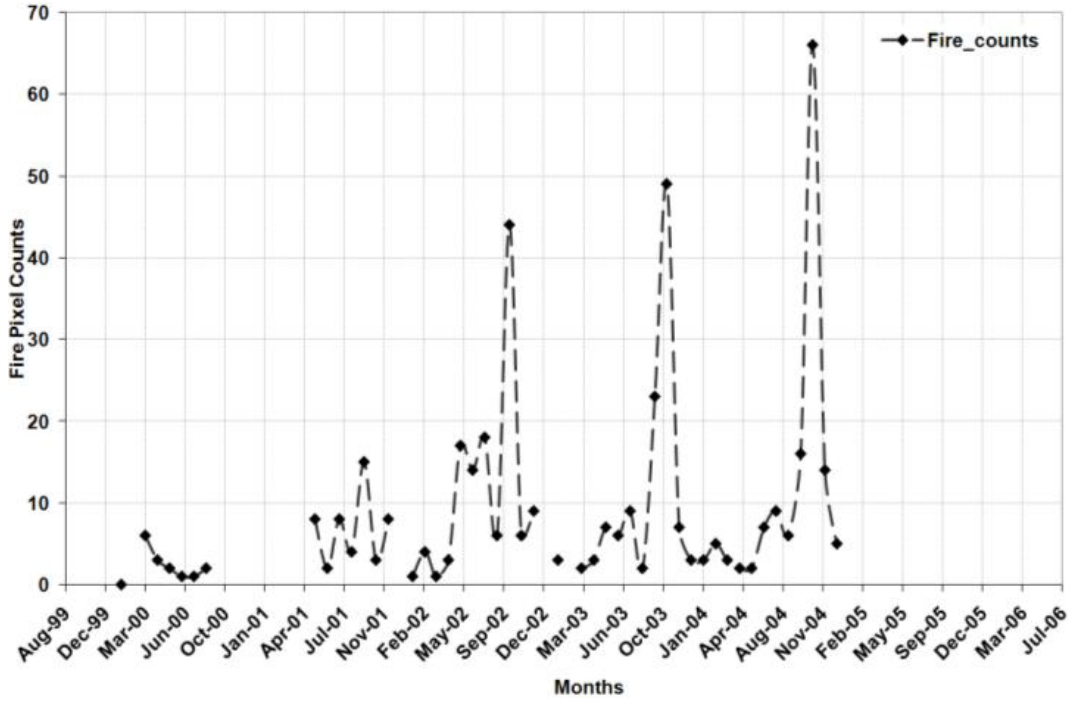


**Fig. 3.** Fire pixel counts in the Greater Nile Delta region as observed by MODIS on Terra, whose average local solar transit time over that location is 8:50 a.m.

namely, dust/pollution/mixed/clean. Some of these days were selected for the back trajectory analysis during 2003, where the GOCART outputs are displayed.

Air-mass back trajectories are typically calculated from gridded meteorological data derived from various sources and archived at regular time intervals each day. A complete description of input data, methodology, equations involved, and sources of error for the air mass trajectory calculations is presented in Draxler and Hess (1997). Figure 4 shows 3-day air-mass back trajectories at three vertical levels ending over Alexandria for the four aerosol categories: dust, pollution, clean, and mixed for highlighted days during 2003 taken from Table 2. The wind directions observed during the dusty days were found to be variable. However, the major dust wind directions were W, S, and SW when the air masses come from the Sahara or North Africa during spring. We observe that when the wind directions are from N and NW, although the origin of the wind may be in Europe, the trajectory passes (typically) over North Africa where the air-mass becomes loaded with dust before reaching Alexandria. Therefore, the air-mass back-trajectory allows for the visualization of a sizeable segment of the air-mass path, giving an indication at where the dust may have been collected from. Dust situations with elevated water-vapor content are often cases where an air mass collects dust from Sahara before or after it collects some moisture over the Mediterranean, after which part of it is blown back by headwinds toward Alexandria. During the pollution days, (summer and fall seasons), the air masses come predominantly from different regions of Eastern, Central or Western Europe mainly due to the well-known convection patterns and the associated prevailing meteorology (Kallos et al., 1998). In other words, elevated $W$ values indicate that the air-mass containing the aerosol probably passed over the Mediterranean to collect moisture before reaching Alexandria. In particular, $W$ is higher during the summer and fall because that is when come predominantly from Europe, gathering moisture over the Mediterranean. Hence, while passing over the Mediterranean toward North Africa, there is a high chance for cloud nucleation and indirect radiative forcing due to the associated sea breeze (El-Askary and Kafatos, 2008). During the days with mixed aerosols, the air masses come from two sources, one that brings pollution from Europe and the other that brings dust from the Sahara and North Africa. The wind directions during the mixed days are from all directions; however, having Westerly flow usually Alexandria is receiving aerosols from the central and western Mediterranean. These different directions reflect the convergence of air masses from diverse source areas. During the clean days, the air masses mainly come from the Atlantic Ocean via the Mediterranean. Therefore, the wind directions during the clean days typically fall between N and W directions. Our outputs have been further corroborated by GOCART model outputs exploring what appears to be significantly high sea salt, dust, sulfates and black carbon concentrations over the Nile Delta region (Fig. 5).

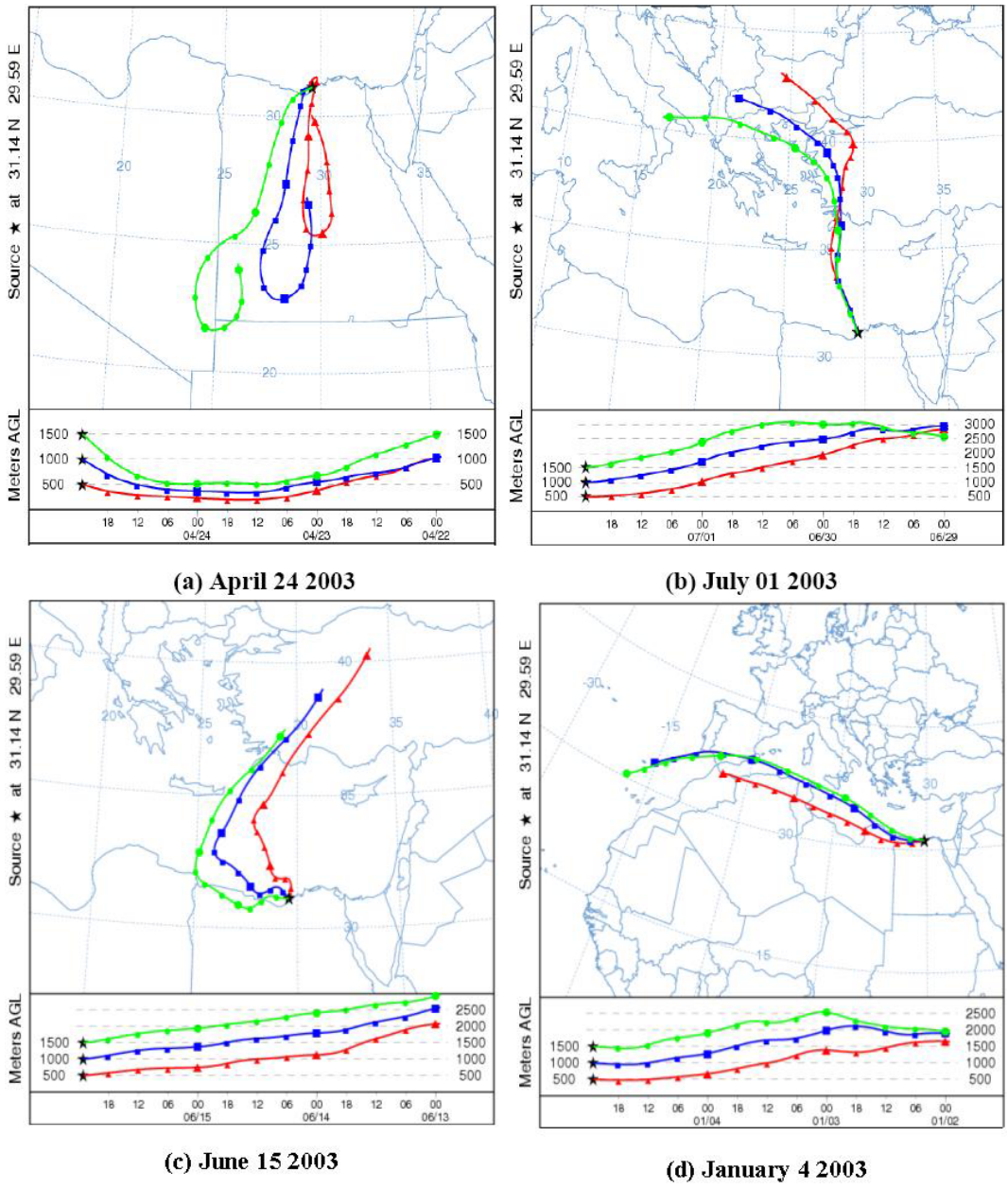


**Fig. 4.** HYSPLIT back-trajectory analysis at different vertical levels (red: 500 m, blue: 1000 m, green: 1500 m) ending over Alexandria showing **(a)** dusty, **(b)** pollution, **(c)** mixed, **(d)** clean conditions in 2003.

## 6 Conclusions

A combination of ground-based and satellite observations were used in this analysis to study different sources of aerosol loadings over Alexandria during two different time periods, namely, October 1999–August 2001, and August 2002–August 2003. Our analysis involved a study of the AOD and associated water vapor column variability, as well as other satellite- derived parameters. Natural versus anthropogenic aerosols are well distinguished using our derived Ångström exponent. We also identified possible mixed and clean atmospheric conditions using the calculated $\alpha_{675/440}$ values. It is clear that dust episodes dominate the spring seasons, as reflected by the high values of AOD associated with sharp drops in the Ångström exponent. Back-trajectory analysis shows agreement with these findings, thereby confirming that the Sahara Desert is the major source of such aerosols during the spring season. Furthermore, the long-range transport of pollutants from Europe during the summer season indicated by model runs is well supported by sharp

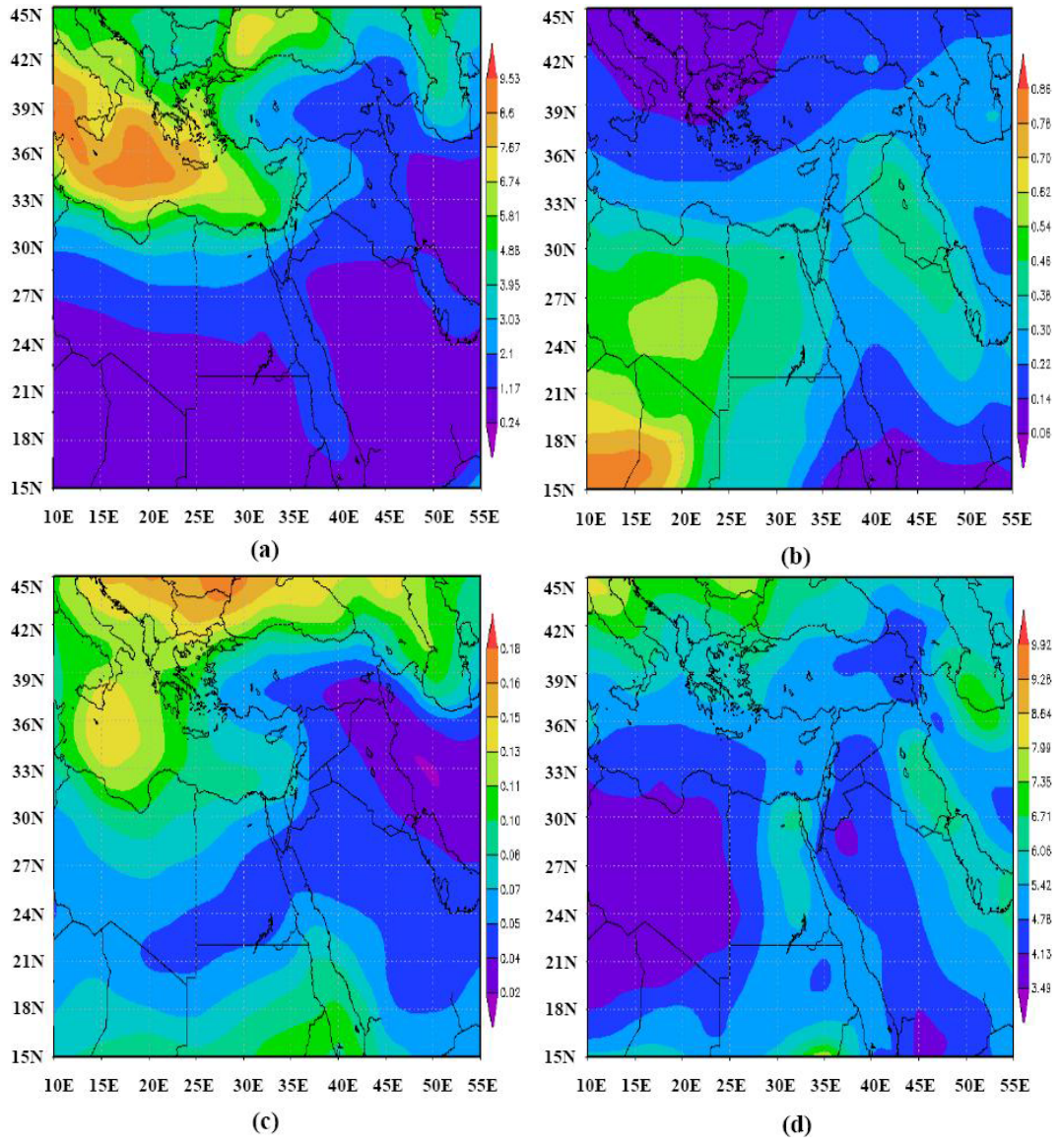


**Fig. 5.** GOCART model outputs of **(a)** sea salt in winter 2003, **(b)** dust in spring 2003, **(c)** sulfates in summer 2003, and **(d)** black carbon AOD in fall 2003 respectively showing potential sources and relative concentrations of these aerosol types over Alexandria and the Nile Delta region.

peaks in the Ångström exponent and corresponding increase in the water-vapor column. Biomass burning and local pollution are most prominent during the fall and winter seasons, as confirmed by the fire pixel counts and the black-carbon concentrations observed from other model outputs. In summary, it is clear that the city of Alexandria and the Greater Nile Delta region are exposed to the impacts of aerosols from various sources throughout the year. This is becoming a serious health hazard because of the persistence of high pollution throughout the year or for prolonged time periods. In addition, the sea-breeze component of the atmospheric circulation brought by the prevailing European trade winds tends to inhibit the development of the land breeze component, thereby allowing the deposition of pollutants from the sky above the city at night, especially during the fall season where the inversion layer is observed to become lower as discussed by El-Askary and Kafatos (2008). This study has demonstrated that long-term measurements of aerosol optical depth (AOD) and precipitable water vapor ($W$) from the ground and from satellite over Alexandria can capture the general transport signal of aerosols from Europe and the Sahara.

**Table 2.** Characterization of the aerosol types over Alexandria, Egypt, for selected dates. Back ward trajectories' are shown for dates in bold (Fig. 5). Shaded cells represent great variations associated with the specified atmospheric scenario in the highlighted parameters.

| Date | $\tau$a675 | $\alpha$675/440 | $W$ |
|---|---|---|---|
| Dust | | | |
| 29 March 2000 | 0.61 | 0.24 | 1.96 |
| 6 April 2000 | 0.55 | 0.12 | 2.51 |
| 1 April 2001 | 0.36 | 0.02 | 1.94 |
| 5 May 2001 | 0.71 | 0.17 | 2.25 |
| 29 September 2002 | 0.31 | 0.22 | 2.86 |
| 10 November 2002 | 0.32 | 0.05 | 1.52 |
| 2 March 2003 | 0.6 | 0.19 | 1.32 |
| **24 April 2003** | **0.82** | **0.08** | **1.77** |
| Pollution | | | |
| 24 August 2000 | 0.18 | 1.29 | 2.66 |
| 20 October 2000 | 0.31 | 1.13 | 3.16 |
| 20 August 2001 | 0.23 | 1.34 | 2.77 |
| 20 September 2002 | 0.15 | 1.29 | 2.32 |
| **1 July 2003** | **0.27** | **1.09** | **3.41** |
| 8 August 2003 | 0.21 | 1.22 | 2.82 |
| Mixed | | | |
| 23 October 1999 | 0.23 | 0.28 | 2.45 |
| 22 February 2000 | 0.14 | 0.36 | 1.79 |
| 29 April 2000 | 0.57 | 0.54 | 2.18 |
| 1 March 2001 | 0.29 | 0.25 | 1.37 |
| 4 April 2001 | 0.09 | 0.85 | 1.70 |
| 30 July 2002 | 0.43 | 0.46 | 2.61 |
| 26 September 2002 | 0.37 | 0.44 | 2.92 |
| 10 March 2003 | 0.28 | 0.88 | 1.77 |
| **15 June 2003** | **0.16** | **0.63** | **2.14** |
| Clean | | | |
| 30 November 1999 | 0.05 | 0.49 | 1.76 |
| 3 January 2000 | 0.05 | −0.22 | 2.21 |
| 23 June 2000 | 0.05 | 0.79 | 1.09 |
| 5 Januray 2001 | 0.05 | 0.81 | 1.64 |
| 9 February 2001 | 0.05 | 0.81 | 1.12 |
| 14 November 2002 | 0.06 | 1.40 | 1.95 |
| **4 January 2003** | **0.04** | **0.63** | **1.04** |
| 17 August 2003 | 0.06 | 1.47 | 1.30 |

*Acknowledgements.* The authors would like also to express their deepest thanks to Ismail Sabbah, Kuwait University, for providing the Microtops instrument used in this study for the data collected by Rania Farouk. Our thanks also go to Mahmoud Gabr, Dean Faculty of science, and Ashraf Ammer, Department of Environmental Sciences, Alexandria University, and Ayman El-Dessouki, Head National Authority of Remote Sensing and Space Sciences, for their continuous help and support. MODIS aerosol and fire data were obtained from the NASA MODIS teams and GOCART model outputs were downloaded from Giovanni Online Visualization and Analysis System operated by the NASA Goddard Earth Sciences Data and Information Services Center (GES DISC). This work is partially funded by the USDA grant 58-3148-7-044, as well as through NASA GEC-hri grant NNX06AF30G and the support from technical officers Don Anderson and Lucia Tsaoussi.

Topical Editor F. D'Andrea thanks four anonymous referees for their help in evaluating this paper.

## References

Alpert, P., Krichak, S. O., Tsidulko, M., Shafir, H., and Joseph, J. H.: A Dust Prediction System with TOMS Initialization, Mon. Weather Rev., 130, 2335–2345, 2002.

Andreae, T. W., Andreae, M. O., Ichoku, C., Maenhaut, W., Cafmeyer, J., Karnieli, A., and Orlovsky, L.: Light scattering by dust and anthropogenic aerosol at a remote site in the Negev desert, Israel, J. Geophys. Res., 107(D2), 4008, doi:10.1029/2001JD900252, 2002.

Ångström, A.: On the atmospheric transmission of sun radiation and on dust in the air, Geogr. Ann., 11, 156–166, 1929.

Badarinath, K. V. S., Shailesh Kumar Kharol, Kaskaoutis, D. G., and Kambezidis, H. D.: Case study of a dust storm over Hyderabad area, India: Its impact on solar radiation using satellite data and ground measurements, Sci. Total Environ., 384(1–3), 316–332, 2007.

Barnaba, F. and Gobbi, G. P.: Aerosol seasonal variability over the Mediterranean region and relative impact of maritime, continental and Saharan dust particles over the basin from MODIS data in the year 2001, Atmos. Chem. Phys., 4, 2367–2391, 2004, http://www.atmos-chem-phys.net/4/2367/2004/.

Charlson, R. J., Langner, J., Rodhe, H., Leovy, C. B., and Warren, S. G.: Perturbation of the northern hemisphere radiative balance by scattering from anthropogenic sulphate aerosols, Tellus A, 43, 152–163, 1991.

Chin, M., Rood, R. B., Lin, S.-J., Muller, J. F., and Thompson, A. M.: Atmospheric sulfur cycle in the global model GOCART: Model description and global properties, J. Geophys. Res., 105, 24671–24687, 2000.

Draxler, R. R. and Hess, G. D.: Description of the HYSPLIT_4 modeling system, NOAA Tech. Memo., ERL ARL-224, 24, 1997.

Draxler, R. R. and Hess, G. D.: An overview of the HYSPLIT_4 modeling system for trajectories, dispersion and deposition, Aust. Meteorol. Mag., 47(4), 295–308, 1998.

Draxler, R. R.: HYSPLIT_4 User's Guide, NOAA Tech. Memo. ERL ARL-230, 35, 1999.

Eck, T. F., Holben, B. N., Reid, J. S., Dubovik, O., Smirnov, A., O'Neill, N. T., Slutsker, I., and Kinne, S.: Wavelength dependence of the optical depth of biomass burning, urban, and desert dust aerosols, J. Geophys. Res., 104, 31333–31349, 1999.

El-Askary, H., Sarkar, S., Kafatos, M., and El-Ghazawi, T.: A multisensor approach to dust storm monitoring over the Nile Delta, IEEE Trans. Geosci. Rem. Sens., 41(10), 2386–2391, 2003.

El-Askary, H.: Air pollution Impact on Aerosol Variability over mega cities using Remote Sensing Technology: Case study, Cairo, Egyp. J. Rem. Sen. Space Sci., 9, 31–40, 2006.

El-Askary, H. and Kafatos, M.: Dust Storm and Black Cloud Influence on Aerosol Optical Properties over Cairo and the Greater Delta Region, Egypt, Int. J. Rem. Sens., 29(24), 7199–7211, 2008.

El-Metwally, M., Alfaro, S. C., Abdel Wahab, M., and Chatenet, B.: Aerosol characteristics over urban Cairo: Seasonal variations as retrieved from Sun photometer measurements, J. Geophys. Res., 113, D14219, doi:10.1029/2008JD009834, 2008.

Gerasopoulos, E., Andreae, M. O., Zerefos, C. S., Andreae, T. W., Balis, D., Formenti, P., Merlet, P., Amiridis, V., and Papastefanou, C.: Climatological aspects of aerosol optical properties in Northern Greece, Atmos. Chem. Phys., 3, 2025–2041, 2003, http://www.atmos-chem-phys.net/3/2025/2003/.

Gobbi, G. P., Kaufman, Y. J., Koren, I., and Eck, T. F.: Classification of aerosol properties derived from AERONET direct sun data, Atmos. Chem. Phys., 7, 453–458, 2007, http://www.atmos-chem-phys.net/7/453/2007/.

Hamonou, E., Chazette, P., Balis, D., Dulac, F., Schneider, X., Galani, E., Ancellet, E., and Papayannis, A.: Characterization of the vertical structure of Saharan dust export to the Mediterranean basin, J. Geophys. Res., 104, 22257–22270, 1999.

Holben, B. N., Eck, T. F., Slutsker, I., Tanre, D., Buis, J. P., Setzer, A., Vermote, E., Reagan, J. A., Kaufman, Y. J., Nakajima, T., Lavenu, F., Jankowiak, I., and Smirnov, A.: AERONET-A federated instrument network and data archive for aerosol characterization, Remote Sens. Environ., 66, 1–16, 1998.

Ichoku, C., Andreae, M. O., Andreae, T. W., Meixner, F. X., Schebeske, G., Formenti, P., Maenhaut, W., Cafmeyer, J., Ptasinski, J., Karnieli, A., and Orlovsky, L.: Interrelationships between aerosol characteristics and light scattering during late- winter in an Eastern Mediterranean arid environment, J. Geophys. Res., 104(24), 371–393, 1999.

Ichoku, C., Levy, R., Kaufman, Y. J., Remer, L. A., Li, R. R., Martins, V. J., Holben, B. H., Abuhassan, N., Slutsker, I., Eck, T. F., and Pietras, C.: Analysis of the performance characteristics of the five-channel Microtops II sun photometer for measuring aerosol optical thickness and precipitable water vapour, J. Geophys. Res., 107(D13), 4179, doi:10.1029/2001JD001302, 2002.

Kallos, G., Kotroni, V., Lagouvardos, K., and Papadopoulos, A.: On the Long-Range Transport of Air Pollutants from Europe to Africa, Geophys. Res. Lett., 25(5), 619–622, 1998.

Kallos, G., Astitha, M., Katsafados, P., and Spyrou, C.: Long-Range Transport of Anthropogenically and Naturally Produced Particulate Matter in the Mediterranean and North Atlantic: Current State of Knowledge, J. Appl. Meteo. Clim., 46(8), 1230–1251, 2007.

Kambezidis, H. D. and Kaskaoutis, D. G.: Aerosol climatology over four AERONET sites: An overview, Atmos. Environ., 42(8), 1892–1906, 2008.

Kaskaoutis, D. G., Kambezidis, H. D., Adamopoulos, A. D., and Kassomenos, P. A.: Comparison between experimental data and modeling estimates of atmospheric optical depth over Athens, Greece, J. Atmos. Solar Terr. Phys., 68, 1167–1178, 2006.

Kaskaoutis, D. G., Kosmopoulos, P., Kambezidis, H. D., and Nastos, P.: Aerosol climatology and discrimination of different types over Athens, Greece based on MODIS data, Atmos. Environ., 41, 7315–7329, 2007.

Kaskaoutis, D. G., Kambezidis, H. D., Nastos, P. T., and Kosmopoulos, P. G.: Study on an intense dust storm over Greece, Atmos. Environ., 42(29), 6884–6896, 2008.

Kaufman, Y. J.: Aerosol optical thickness and atmospheric path radiance, J. Geophys. Res., 98(D2), 2677–2692, 1993.

Kiehl, J. T. and Rodhe, H.: Modeling geographical and seasonal forcing due to aerosols, in: Aerosol Forcing of Climate, edited by: Charlson, R. J. and Heintzenberg, J., J. Wiley, New York, 281–296, 1995.

King, M. D., Byrne, D. M., and Herman, B. M.: Aerosol size distribution obtained by inversion of spectral optical depth measurements, J. Atmos. Sci., 35, 2153–2167, 1978.

Kouvarakis, G., Doukelis, Y., Mihalopoulos, N., Rapsomanikis, S., Sciare, J., and Blumtharel, M.: Chemical, physical and optical characterization of aerosols during PAUR II experiment, J.Geophys. Res., 107(D18), 8141, doi:10.1029/2000JD000291, 2002.

Lelieveld, J., Berresheim, H., Borrmann, S., Crutzen, P. J., Dentener, F. J., Fischer, H., Feichter, J., Flatau, P. J., Heland, J., Holzinger, R., Korrmann, R., Lawrence, M. G., Levin, Z. Markowicz, K. M., Mihalopoulos, N. Minikin, A. Ramanathan, V., de Reus, M., Roelofs, G. J., Scheeren, H. A., Sciare, J., Schlager, H., Schultz, M., Siegmund, P., Steil, B., Stephanou, E. G., Stier, P., Traub, M., Warneke, C., Williams, J., and Ziereis, H.: Global air pollution crossroads over the Mediterranean, Science, 298, 794–799, 2002.

Levy, R. C., Remer, L. A., Mattoo, S., Vermote, E. F., and Kaufman, Y. J.: Second-generation operational algorithm: Retrieval of aerosol properties over land from inversion of Moderate Resolution Imaging Spectroradiometer spectral reflectance, J. Geophys. Res., 112, D13211, doi:10.1029/2006JD007811, 2007.

Luria, M., Peleg, M., Sharf, G., Tov-Alper, D., Spitz, N., Ben Ami, Y., Gawii, Z., Lifschitz, B., Yitzchaki, A., and Seter, I.: Atmospheric sulfur over the east Mediterranean region, J. Geophys. Res., 101(D20), 25917–25930, 1996.

Meloni, D., di Sarra, A., Monteleone, F., Pace, G., Piacentino, S., and Sferlazzo, D.M.: Seasonal transport patterns of intense Saharan dust events at the Mediterranean island of Lampedusa, Atmos. Res., 88(2) 134–148, 2008.

Millan, M. M., Salvador, R., Mantilla, E., and Kallos, G.: Photo oxidant dynamics in the Mediterranean basin in summer: results from European research projects, J. Geophys. Res., 102, 8811–8823, 1997.

Moulin, C., Lambert, C. E., Dayan, U., Masson, V., Ramonet, M., Bousquet, P., Legrand, M., Balkanski, Y. J., Guelle, W., Marticorena, B., Bergametti, G., and Dulac, F.: Satellite climatology of African dust transport in the Mediterranean atmosphere, J. Geophys. Res., 103, 13137–13144, 1998.

Nakajima, T., Takamura, T., and Yamano, M.: Consistency of aerosol size distributions inferred from measurements of solar radiation and aerosols, J. Met. Soc. Jap., 64, 765–776, 1986.

O'Neill, N. T., Dubovik, O., and Eck, T. F.: A modified Ångström coefficient for the characterization of sub-micron aerosols, Appl. Optics, 40, 2368–2375, 2001a.

O'Neill, N. T., Eck, T. F., Holben, B. N., Smirnov, A., and Dubovick, O.: Bimodal size distribution influences on the variation of Ångström derivatives in spectral and optical depth space, J. Geophys. Res., 106(D9), 9787–9806, 2001b.

O'Neill, N. T., Eck, T. F., Smirnov, A., Holben, B. N., and Thulasiraman, S.: Spectral discrimination of coarse and fine mode optical depth, J. Geophys. Res., 108(D17), 4559,

doi:10.1029/2002JD002975, 2003.

Paronis, D., Doulac, F., Chazette, P., Hamonou, E., and Liberti, G. L.: Aerosol optical thickness monitoring in the Mediterranean, J. Aerosol Sci., 30, 631–632, 1998.

Piketh, S. J. and Walton, N. M.: Characteristics of atmospheric transport of air pollution for Africa, in Intercontinental Transport of Air Pollution, Handb. Environ. Chem., Springer, New York, 4G, 173–195, 2004.

Pinker, R. T., Ferrare, R. A., Karnieli, A., Aro, T. O., Kaufman, Y. J., and Zangvil, A.: Aerosol optical depths in a semiarid region, J. Geophys. Res., 102(11), 123–137, 1997.

Prasad, A. K. and Singh, R. P.: Changes in aerosol parameters during major dust storm events (2001–2005) over the Indo-Gangetic Plains using AERONET and MODIS data, J. Geophys. Res., 112, D09208, doi:10.1029/2006JD007778, 2007.

Ramachandran, S.: Spectral aerosol optical characteristics during the northeast monsoon over the Arabian Sea and the tropical Indian Ocean: 2. Ångström parameters and anthropogenic influence, J. Geophys. Res., 109, D19208, doi:10.1029/2003JD004476, 2004.

Remer, L. A., Kaufman, Y. J., Tanré, D., Mattoo, S., Chu, D. A., Martins, J. V., Li, R.-R., Ichoku, C., Levy, R. C., Kleidman, R. G., Eck, T. F., Vermote, E., and Holben, B. N.: The MODIS aerosol algorithm, products and validation., J. Atmos. Sci., 62(4), 947–973, 2005.

Sabbah, I., Ichoku, C., Kaufman, Y. J., and Remer, L. A.: Full year cycle of desert dust spectral optical thickness and precipitable water vapor over Alexandria, Egypt, J. Geophys. Res., 106, 18305–18316, 2001.

Schuster, G. L., Dubovick, O., and Holben, B. N.: Ångström exponent and bimodal aerosol size distributions, J. Geophys. Res., 111, D07207, doi:10.1029/2005JD006328, 2006.

Singh, S., Nath, S., Kohli, R., and Singh, R.: Aerosols over Delhi during pre-monsoon months: Characteristics and effects on surface radiation forcing, Geophys. Res. Lett., 32, L13808, doi:10.1029/2005GL023062, 2005.